Journal of Visualization, Vol. 7, No. 4 (2004) 309-316

Visualization of Three-Dimensional Flow Structures in the Wake of an Inclined Circular Cylinder

Matsuzaki, K.*1, Shingai, M.*1, Haramoto, Y.*2, Munekata, M.*1 and Ohba, H.*1

*1 Dept. of Mechanical Engineering and Materials Science, Kumamoto University, 2-39-1 Kurokami, Kumamoto, 860-8555, Japan. E-mail: mzaki@gpo.kumamoto-u.ac.jp
*2 Mitsui Miike Machinery Co., LTD, 2-28 Asahi-machi, Ohmuta, Fukuoka , 836-8588, Japan.

Received 21 September 2003
Revised 30 June 2004

Abstract : In the previous measurements of the aerodynamic sound generated from an inclined circular cylinder, it is reported that the sound pressure level (SPL) changes with the aspect ratio and the inclined angle. Therefore, we have investigated the changes in the vortex structure of the wake considered as one of the causes of the SPL variation. Using the low-noise wind tunnel, the velocity fluctuation in the wake is measured to obtain the correlation length. Moreover, the flow visualization is performed with a hydrogen bubble method and a numerical analysis method in order to clarify how the wake structure changes by variations of aspect ratio and inclined angle. As a result of this investigation, it is shown that the spanwise structure of Karman's vortex is highly influenced by the interference of Karman's vortex with the bottom endplate, and that the influence on the spanwise structure in the wake becomes greater as the aspect ratio decreases and the inclined angle increases.

Keywords : Wake, Aerodynamic sound, Correlation length, Hydrogen bubble method, Numerical analysis, Flow visualization.

1. Introduction

Public concerns about the environment have increased in recent years and noise reduction from the production devices such as fluid machineries, electronics devices, transport vehicles and so on is becoming more important than ever before. Therefore, it is a very important issue for the researchers and the developers to reduce the generated noise and to control the discordant noise. In particular, such aerodynamic noise problems have increased rapidly. For the design of such production devices, it is essential to clarify the generation mechanism of the aerodynamic sound from a two-dimensional body such as circular cylinders, square cylinders, airfoils and so on.

Most of measurements in the aerodynamic sound generated from the two-dimensional bodies have been performed on the condition that the attack angle and the inclined angle are zero. For the practical applications, it is very important to grasp the influences of them on the generated sound. For the typical two-dimensional bodies such as the circular cylinder and the square cylinder, Yamada et al. (1997) experimentally examined the influences of the inclined angle for the circular cylinder and the attack angle of the square cylinder on the generated aerodynamic sound with the low noise wind tunnel. Haramoto et al. (2001) focused on the inclined angle for the circular cylinder and the aspect ratio, which is defined as the ratio of the distance between acoustically transparent endplates to the cylinder diameter, and experimentally studied their influences on the generated aerodynamic sound in the low noise wind tunnel. However, in those experimental works, the causes of the change of the aerodynamic sound with the inclined angle and the attack angles are not fully discussed. Since it is considered that the aerodynamic sound highly depends on the flow structures, it is very important to investigate them. It is reported that the correlation length of a large scale vortex in the spanwise direction, which is one of factors in evaluating a scale of the flow structure, plays an important role for analyzing the aerodynamic noise (Iida, et al., 1995, Kato, et al., 1994). Moreover, Shirakashi et al. (1986) have experimentally investigated the structure of Karman's vortex shedding from a yawed cylinder in a uniform flow, and reported that a secondary flows along the axis of the cylinder lead to the reductions in the frequency and the regularity of the vortex shedding as the inclined angle increases.

In this paper, we focused on the inclined circular cylinder and investigated the spanwise changes in the vortex structure of the wake considered as one of the causes of the change of aerodynamic sounds. Using the low-noise wind tunnel, we measured the velocity fluctuation in the wake to obtain the correlation length. Moreover, the flow visualization is performed with a hydrogen bubble method and a numerical analysis method in order to clarify how the spanwise structures of the wake change with the inclined angle and the aspect ratio. From the investigation, the relationship between the changes of the aerodynamic sound with an inclined angle and an aspect ratio and the spanwise changes in the vortex structure of the wake in the inclined circular cylinder is discussed.

2. Experimental and Numerical Method

2.1 Experiment Using Low Noise Wind Tunnel

The measurements of the sound pressure and the velocity fluctuation in the wake were performed in the low noise wind tunnel belonging to the Mitsui Miike Machinery Co., LTD. The wind tunnel with a circuit and semi-open type, has an open test section of 0.3 m × 0.3 m. The flow noise level is less than 55 dB (A) and the turbulence level is less than 0.2 % at a velocity of 40 m/s. The endplates were installed in the test section because in an open type wind tunnel, interference between the large scale turbulence in the jet edge and the model generates unexpected additional aerodynamic noise and destroys the two-dimensionality of the flow around the model (Fujita et al., 1996). The circular cylinder was set up as shown in Fig. 1(a). The bottom of the cylinder was fixed at 65 mm position from the nozzle end. The upper end could be slid in the downstream direction to set arbitrarily the inclined angle ψ. For the coordinate system, the origin was the center of a cylinder, X, Y and Z were the downstream, horizontal and vertical direction respectively. As shown in Fig. 1(a), the aspect ratio A is defined by the ratio of distance between endplates H and cylinder diameter d. It can vary with the cylinder diameter. The sound pressure was measured by a sound level meter that was set perpendicular to both the cylinder axis and streamwise direction, at a distance of 1 m from the center of the cylinder (Fig. 1(b)).

We measured the correlation length with two standard hot-wire sensors, which is tungsten wire with a diameter of 5 μ m, in the wake behind the cylinder. As shown in Fig. 1(c), one of the two hot-wire sensors was fixed at (X, Y, Z)=(1.5d, 2.5d, 0) and the other was traversed parallel to the cylinder axis at intervals of 4 mm. The correlation length was calculated by the following equations.

$$L_c = \frac{L_c'(L-\gamma)}{L} \tag{1}$$

$$L_c' = 2\int_0^L r(z)dz\ ,\quad \gamma = \int_0^L z\,r(z)\,dz \ /\ \int_0^L r(z)\,dz \tag{2}$$

where r, z, γ, L and L_c' represent the cross correlation coefficient, the distance between the two hot-wire sensors, the position of the centroid of the correlation area, the value of z position at r=0 and the correlation length defined by Blevins (1990), respectively. However, in this paper, we used L_c in equation (1) as the correlation length instead of L_c', because the correlation length L_c should contain the position of centroid of the correlation area γ. The measurement of the correlation length was conducted on the condition that the Reynolds number based on the velocity of main stream V and the circular cylinder is fixed at 20,000. Then, the aspect ratio was set at 10, 15 and 30, the inclined angle of the circular cylinder at 0º and 20º.

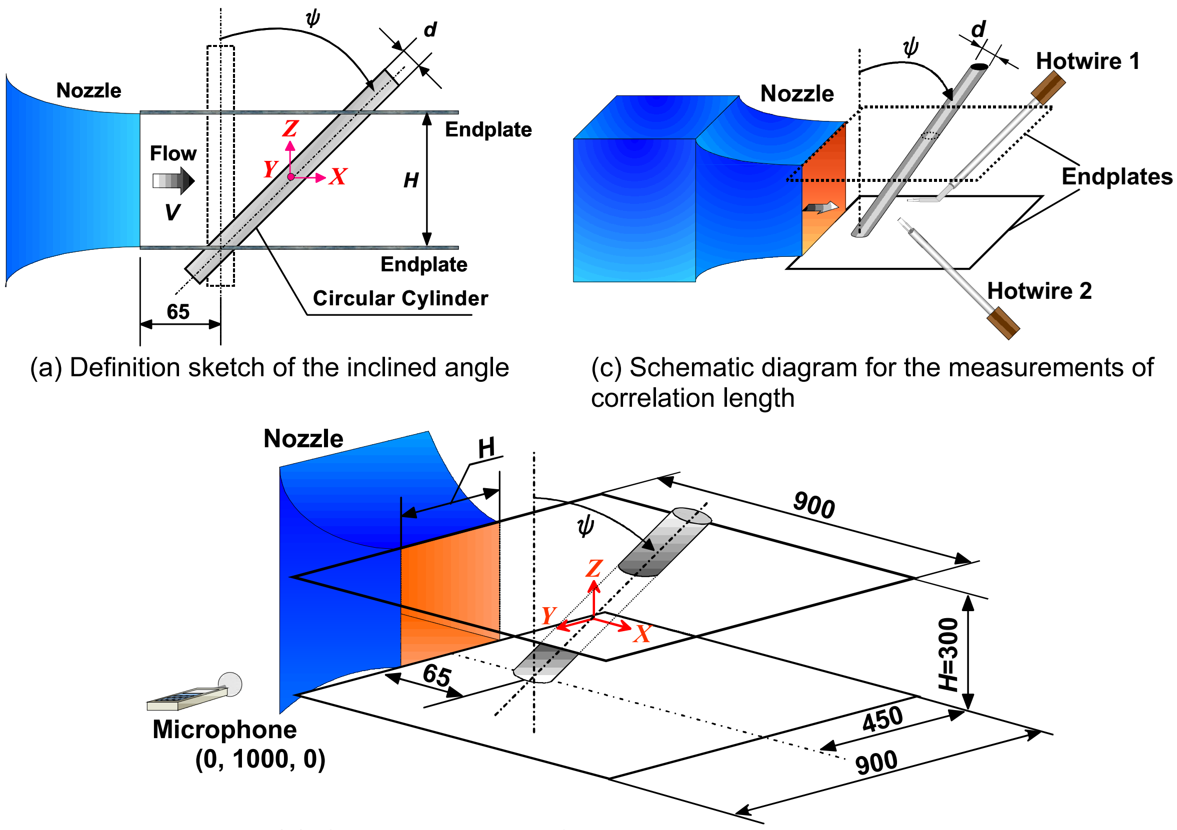

(a) Definition sketch of the inclined angle

(c) Schematic diagram for the measurements of correlation length

(b) Schematic diagram for the noise measurements

Fig. 1. Schematic diagram of the experimental setup.

2.2 Flow Visualization Using Hydrogen Bubble Method

Figure 2 shows the experimental apparatus for the flow visualization using the hydrogen bubble method. It is a circuit-type water tunnel and the flow enters the observation section after the large scale turbulence is removed by honeycombs and screens. The observed section with a length of 1000 mm, a height of 200 mm and a width of 200 mm is made of acrylic acid resin. The circular cylinder was fixed in the endplate unit and was immersed in the observation section. The hydrogen bubbles were generated from the surface of the circular cylinder that was made of brass and shot from the side. The experiments were performed with Reynolds number 450. The velocity of the main stream, the cylinder diameter and the water temperature were 0.09 m/s, 4 mm and 30°, respectively. The aspect ratio can be varied with the distance between the endplates. The Reynolds number in the flow visualization is different from that in the experiment with the low noise wind tunnel. However, we suppose that the effect of the difference in Reynolds number on the flow around the circular cylinder is very small, because $300 < Re < 20{,}000$ is a range of sub-critical Reynolds number and the flow around the circular cylinder shows laminar separation in this range. The range of the inclined angle was from 0° to 30°, in intervals of 10°. The aspect ratio was set at 10, 15 and 30.

2.3 Numerical Analysis Method

The governing equations for incompressible flow are Navier-Stokes equations and the continuity equation. The finite-difference method was used for the discretization. A fractional step method was used for the solution of the pressure. The convective terms were discretized with 3rd-order up-wind scheme (Kawamura and Kuwahara, 1984) and all spatial terms except them were discretized with 2nd-order central difference scheme. In the time integration, the 2nd-order Adams-Bashforth method was applied to the convective terms. The 2nd-order Crank-Nicolson method was used for the

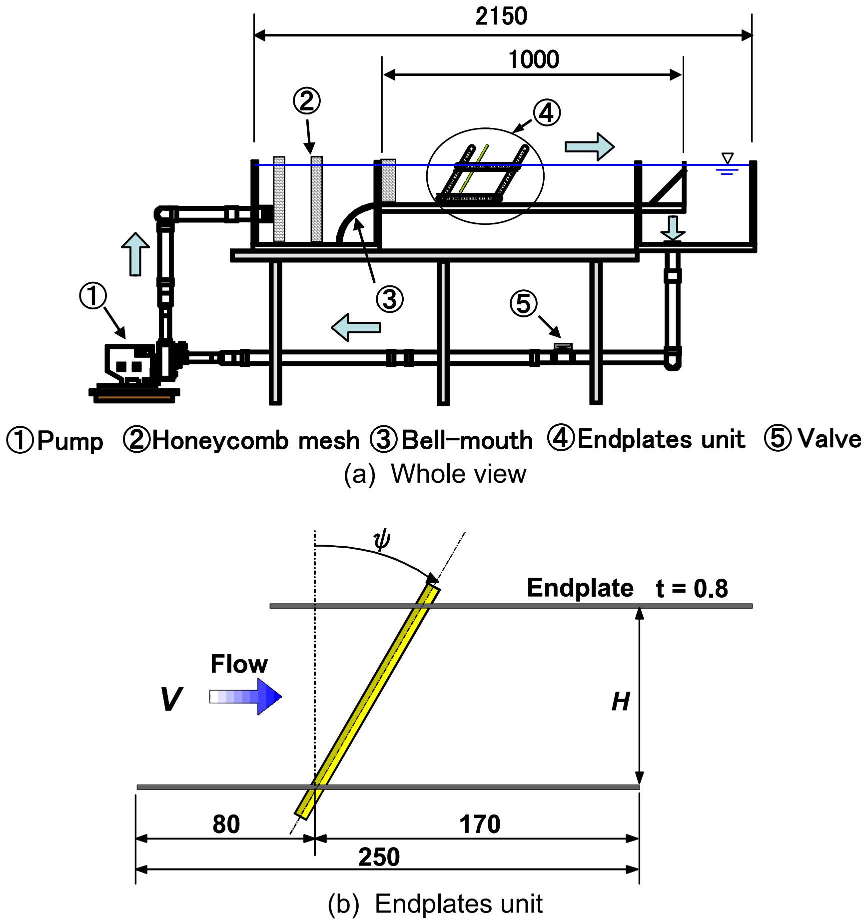

Fig. 2. Experimental apparatus for the flow visualization using the hydrogen bubble method.

viscous terms. A regular grid system with O-type topology was used. The dimensionless time increment Δt and the minimum grid width are taken to satisfy the condition that the courant number is less than 1.0 throughout all the calculation domain. Neumann conditions are imposed on pressure at the solid walls. Non-slip conditions are used for velocities on the walls. The uniform flow is given for far upstream boundary, and gradient free condition was imposed on the far downstream boundary. In this simulation, the computational domain has an outer boundary of $30d$ and a height of $10d$. The numbers of grid points are 53 in the radial direction, 101 in the circumferential direction and 84 in the axial direction. The Reynolds number was set at 450 corresponding to that of the flow visualization. The range of the inclined angles was from 0° to 30°, in intervals of 10°.

3. Results and Discussion

3.1 Characteristics of the Aerodynamic Sound for the Inclined Circular Cylinder

Figure 3 shows the effect of the inclined angle on the band level BL. The band level is a sound pressure level considering the frequency and peak level of prominent spectra, probably caused by Karman's vortex shedding and is calculated by the method based on that of Yamada et al. (1997). In A=30, BL slightly increases with the increase of the inclined angle and has maximum value at about 20°, and then decreases as the inclined angle increases. On the other hand, in A=15 and 10, BL decreases with increasing inclined angle. BL decreases rapidly in A=15 when the inclined angle exceeds 10°, while BL in A=10 decreases rapidly at $\psi > 5°$. BL in A=10 increases with the inclined angle from 20° to 30°. From the spectra of the sound pressure level, it can be seen that the peak

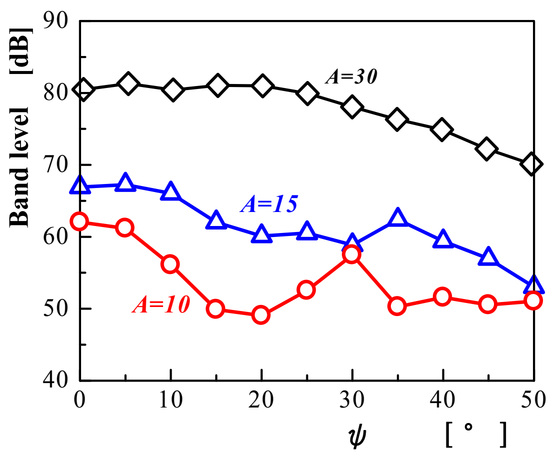

Fig. 3. Effect of inclined angle on the band level.

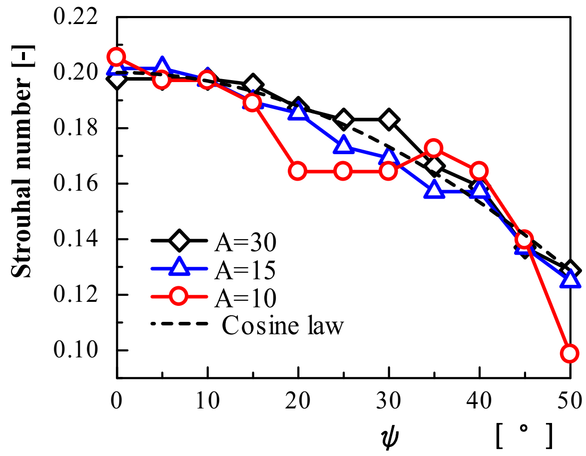

Fig. 4. Effect of inclined angle on Strouhal number.

Table 1. Dimensionless correlation length α.

	A=30	A=15	A=10
ψ=0°	3.5	2.8	1.9
ψ=20°	4.9	1.9	1.7

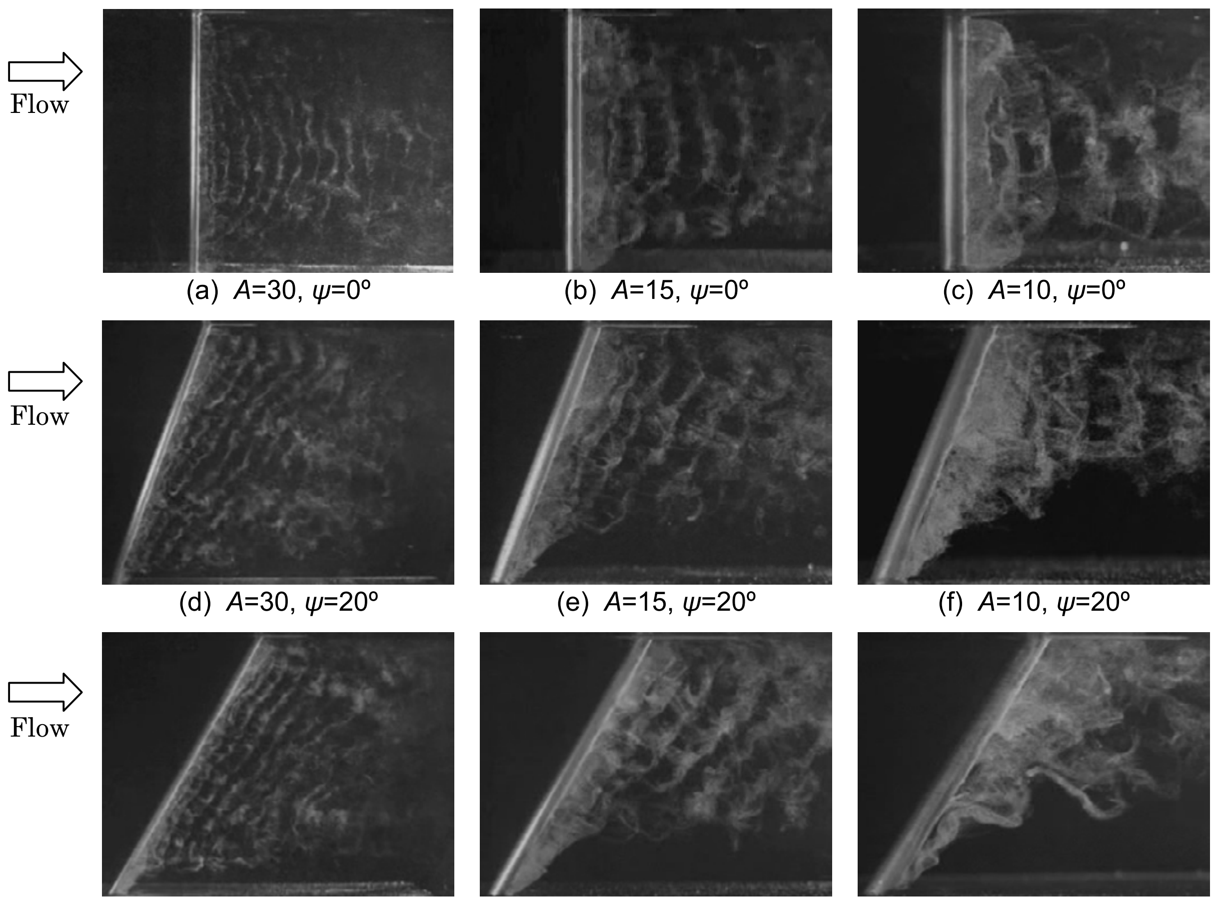

(a) A=30, ψ=0° (b) A=15, ψ=0° (c) A=10, ψ=0°

(d) A=30, ψ=20° (e) A=15, ψ=20° (f) A=10, ψ=20°

(g) A=30, ψ=30° (h) A=15, ψ=30° (i) A=10, ψ=30°

Fig. 5. Snapshots of the wake behind the circular cylinder obtained from the flow visualization using the hydrogen bubble method (Re=450).

spectrum in ψ=30° is wider than that in ψ=20°, and that the peak level in ψ=30° is higher than that in ψ=20°. It is considered that the increase in BL at ψ=30° is attributed to the instability of Karman's vortex in the wake. Figure 4 shows the profile of Strouhal number based on the peak frequency in the spectra of sound pressure level and the velocity of main stream V From this figure, it is found that the Strouhal number decreases as the inclined angle increases. It is well known that the frequency of vortex shedding in an inclined cylinder follows the cosine law (Van Atta, 1968). However, the Strouhal number in A=10 highly deviates from the law at ψ >15°. Table 1 shows the dimensionless correlation length α (=L_c/d) obtained from the velocity fluctuation along the spanwise direction in the wake behind the circular cylinder. In A=30, the dimensionless correlation length at ψ=20° is longer than that at ψ=0°. On the other hand, in A=10 and 15, the dimensionless correlation length at ψ=20° is shorter than that at ψ=0°. The decrease in the non-dimensional correlation length probably means the reduction of the spanwise regularity in Karman's vortex, and this would be related to the decrease in BL.

3.2 Flow Visualization of the Wake by Hydrogen Bubble Method

The snapshots of the flow visualization measured by the hydrogen bubble method are shown in Fig. 5. In ψ=0°, the regular vortex shedding can be observed, and the arched-shaped vortex is formed in the spanwise direction due to the lower velocity near the endplates. In ψ=20°, the vortex shedding along the axis of the cylinder can be seen. However, the vortex shedding near the bottom endplate delays and the axis of Karman's vortex is slightly slanted to that of the cylinder. The interference of Karman's vortex with the bottom endplate becomes greater as the aspect ratio is smaller. For A=10, the axis of the vortex becomes almost parallel to the spanwise direction. This is probably due to the influence of the upper endplate. In ψ=30°, it is found that the interference with the bottom endplate becomes greater. For A=10, the heaving upward flow from the bottom endplate can be seen, and the regular vortex street can be no longer observed.

It is reported that a secondary flow along the cylinder axis, which corresponds to the upward flow from the bottom endplate to the upper endplate in this study, is formed behind the cylinder when the yawed cylinder is placed in a uniform flow (Shirakashi et al., 1986, Kawamura and Hayashi, 1994). This means that only the inclination of cylinder causes the upward flow along the axis of the cylinder. As the inclined angle is larger, the interference of the upward flow with the bottom endplate becomes greater and highly influences the wake structure. In A=15 and 30, it is confirmed that the spanwise structure of Karman's vortex is not broken down by the interference. However, that in ψ=30° is done in A=10. It is considered that the change in the spanwise structure of Karman's vortex due to the interference highly influences that in BL with variations of the inclined angles and the aspect ratios. Moreover, for the larger aspect ratio, it seems that the spanwise structure of Karman's vortex becomes stronger as the inclined angle increases (see Figs. 5(a), (d) and (g)). This tendency corresponds to that of the dimensionless correlation length obtained from the velocity fluctuation.

3.3 Flow Visualization Obtained from Numerical Simulation

Figure 6 shows the instantaneous flow obtained from the numerical simulation behind the circular cylinder near the bottom endplate at ψ=0° and 20°. In this figure, the streamlines and the iso-surface in the spanwise velocity w=0.5 are shown and the pressure distributions are mapped on the iso-surface. In ψ=0°, it can be seen that the complicated flow is generated by the interference of Karman's vortex with the bottom endplate behind the cylinder. The region with the high spanwise velocity becomes larger as the inclined angle increases. Moreover, it is observed that the horseshoe vortex seen near the bottom endplate rolls up behind the circular cylinder, and interferes with Karman's vortex. This interference becomes stronger as the inclined angle increases. Thus, it is suggested that the upward flow along the cylinder axis caused by only the inclination of cylinder interferes with the horseshoe vortex behind the cylinder and the interference probably develops the stronger upward flow. This would break down the spanwise structure of Karman's vortex.

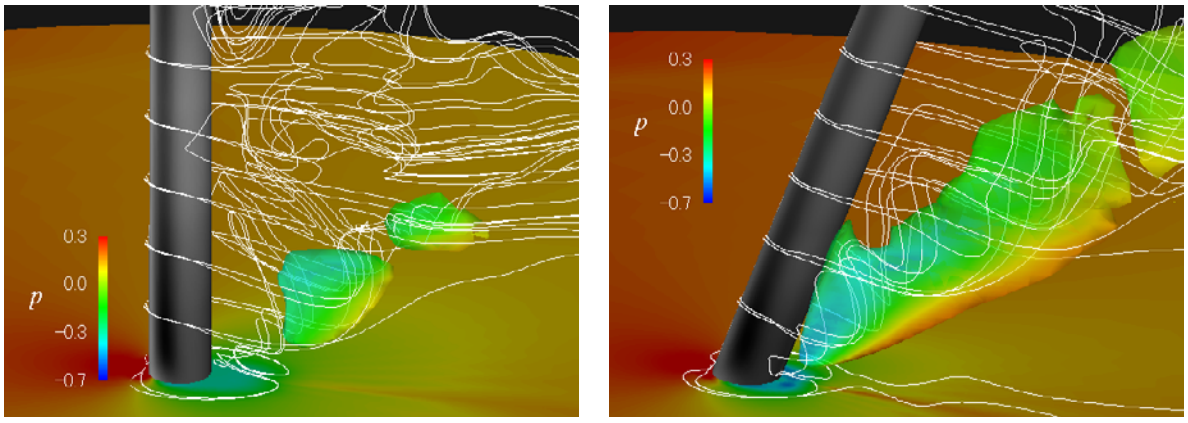

(a) ψ=0° (b) ψ=20°

Fig. 6. Snapshots obtained from the numerical simulation (Re=450, A=10); Streamlines are obtained from the instantaneous velocity. The volume behind cylinder indicates the iso-surface with the instantaneous velocity component w=0.5 in the z direction. The color bar shows the value of the instantaneous pressure.

4. Conclusion

In this paper, we focused on the inclined circular cylinder and investigated the spanwise changes in the vortex structure of the wake considered as one of the causes of the change of the aerodynamic sound. From the measurements in the spanwise correlation length of the wake using the low-noise wind tunnel, in A=30, it is found that the structure of Karman's vortex becomes stronger in the direction of the cylinder axis as the inclined angle increases. On the other hand, in A=10 and 15, it becomes smaller with the increase of the inclined angle. This would be related to the decrease in BL. From the flow visualization of the wake by the hydrogen bubble method, it is confirmed that the strong upward flow due to interference of Karman's vortex with the bottom endplate influences on the spanwise structure. This influence becomes more remarkable as the aspect ratio is smaller and the inclined angle is larger. From the flow visualization obtained by the numerical simulation behind the circular cylinder near the bottom endplate, it is suggested that the upward flow along the cylinder axis caused by only the inclination of cylinder interferes with the horseshoe vortex behind the cylinder and the interference probably develops the stronger upward flow. This would break down the spanwise structure of Karman's vortex. The variation in BL is related to the spanwise structure of Karman's vortex and can be estimated by the correlation length. However, for the smaller aspect ratio and larger inclined angle (A=10 and ψ=30°), the increase in BL cannot be accounted for by only the spanwise structure due to the complicated wake with strong three-dimensionality.

References

Blevis, R. D., Flow-Induced Vibration Second Edition, Van Nostrand Reinhold, New York, (1990), 349-359.

Fujita, H., Shiraishi, J., Kurita, K., Maruta, Y. and Yamada, S., Experimental Study on Aerodynamic Noise Generated from Two-dimensional Models (1st Report, Study on Wind Tunnel Wall Effect and Wall Materials), Trans. of JSME, (B), 62-593 (1996), 187-193. (in Japanese)

Haramoto, Y., Yasuda, S., Matsuzaki, K., Munekata, M. and Ohba, H., Effect of Aspect Ratio on Aerodynamic Sound Generated from Inclined Circular Cylinder, The Proceedings of 7th AIAA/CEAS Aeroacoustic Conference, AIAA 2001-2248 (2001).

Iida, A., Fujita, H., Kato, C. and Takano, Y., Experimental Investigation of Generation Mechanism of Aerodynamic Noise (1st Report, On a Coherent Structure of Surface Pressure Fluctuation on a Circular Cylinder), Trans. of JSME, (B), 61-592 (1995), 4371-4378. (in Japanese)

Kato, C., Takano, Y., Iida, A. Fujita, H. and Ikegawa, M., Numerical Prediction of Aerodynamic Sound by Large Eddy Simulation (1st Report, Aerodynamic Sound Radiated from Two-Dimensional Circular Cylinder), Trans. of JSME, (B), 60-569 (1994), 26-132. (in Japanese)

Kawamura, T. and Hayashi, T., Computation of Flow around a Yawed Circular Cylinder, JSME International Journal Series B, 37-2 (1994), 229-236.

Kawamura, T. and Kuwahara, K., Computational of High Reynolds Number Flow around a Circular Cylinder with Surface Roughness, AIAA Paper No.84-0340 (1984).

Shirakashi, M., Isono, M. and Wakita, S., Structure of Karman Vortex Shedding from a Yawed Cylinder in a Uniform Flows,

Trans. of JSME, (B), 52-481 (1986), 3152-3158. (in Japanese)
Yamada, S., Fujita, H., K., Maruta, Y. Maki, H. and Shiraishi, J., Experimental Study on Aerodynamic Noise Generated from Two-dimensional Models (2nd Report, Effect of the Angle of Inclination of Circular Cylinders and the Angle of Attack of Square Cylinders to Aerodynamic Noise), Trans. of JSME, (B), 63-610 (1997), 1974-1979. (in Japanese)
Van Atta, C. W., Experiments in Vortex Shedding from Yawed Circular Cylinders, AIAA Journal, 6-5 (1968), 931-933.

Author Profile

Kazuyoshi Matsuzaki: He received his MSc (Eng.) and Ph. D. from Kumamoto University in 1995 and 1998, respectively. He has been working for Kumamoto University in the Department of Mechanical Engineering and Materials Science since 1998 as a research associate. His research interests are computational fluid dynamics in turbulent flows, aerodynamic sound generated from 2-dimensional bodies and flow visualization.

Mitsuru Shingai: He received his MSc (Eng.) in Mechanical Engineering in 2003 from Kumamoto University. He experimentally worked aerodynamic sound generated from 2-dimensional bluff bodies and airfoils in the Fluid Machinery Laboratory. Now he works as an engineer at HONDA MOTOR CO., LTD. after obtaining his MSc.

Yasutake Haramoto: He received his M., M. (Eng.) degree in Mechanical Engineering in 1996 from Kumamoto University and his Ph.D. in Mechanical Engineering in 2002 from the same university. After obtaining M., M., he started to work as an engineer in a hydromachine design group at Mitsui Miike Machinery Co., LTD. He then changed his job to aero-dynamist in Motor Sports Division at TOYOTA MOTOR CORPORATION. His current research interests are computational fluid dynamics, wind tunnel experiment and aerodynamic development of formula-one car.

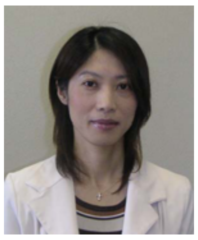

Mizue Munekata: She received her BS in Chemistry in 1994 from Kumamoto University. She also received her Ph.D. in Mechanical Engineering in 2002 from Kumamoto University. She works in Kumamoto University since 1994 and currently is a research associate. Her current research interests are drag-reducing flow, non-Newtonian fluid flow and quantitative flow visualization.

Hideki Ohba: He received his M. Eng. in Resource Development Engineering in 1968 from Kumamoto University. He also received his D. Eng. in Mechanical Engineering in 1982 from Kyusyu University. He works in Kumamoto University since 1968 and currently is a professor. His current research interests are internal flow in rotational fluid machinery, computational fluid dynamics and quantitative flow visualization.